Optical Properties of Individual Silicon Nanowires for Photonic Devices

Gerald Brönstrup,[†,*] Norbert Jahr,[†] Christian Leiterer,[†] Andrea Csáki,[†] Wolfgang Fritzsche,[†] and Silke Christiansen[†,‡]

[†]Institute of Photonic Technology Jena, 07745 Jena, Germany, and [‡]Max Planck Institute for the Science of Light, 91058 Erlangen, Germany

ARTICLE

ABSTRACT Silicon is a high refractive index material. Consequently, silicon nanowires (SiNWs) with diameters on the order of the wavelengths of visible light show strong resonant field enhancement of the incident light, so this type of nanomaterial is a good candidate for all kinds of photonic devices. Surprisingly enough, a thorough experimental and theoretical analysis of both the polarization dependence of the absorption and the scattering behavior of individual SiNWs under defined illumination has not been presented yet. Here, the present paper will contribute by showing optical properties such as scattering and absorption of individual SiNWs experimentally in an optical microscope using bright- and dark-field illumination modes as well as in analytical Mie calculations. Experimental and calculation results are in good agreement, and both reveal a strong correlation of the optical properties of individual SiNWs to their diameters. This finding supports the notion that SiNWs can be used in photonic applications such as for photovoltaics or optical sensors.

KEYWORDS: silicon · nanowire · optics · individual spectra · scattering · absorption · Mie

Silicon nanowires (SiNWs) in ensembles, usually on large area substrates such as wafers or glass sheets, have attracted much attention in the past few years to potentially serve as future building blocks in sensors,[1] transistors,[2] solar cells,[3−7] and photodetectors.[8,9] A prerequisite for using SiNWs in the aforementioned devices is that the electrical and optical properties are understood and can be controlled. So far, neither the understanding nor the control is satisfying. The present paper tries to support an enhanced understanding of the optical properties of individual SiNWs.

Many papers have been published dealing with the optical properties of nanowire (NW) ensembles.[10−15] A major part of the analysis of the measured data therein is based on the scattering properties of individual NWs in the Rayleigh limit, which is valid for diameters $d \ll \lambda/(\pi n)$.[16] Furthermore, non-Rayleigh-type resonances for these systems have been reported.[13] The knowledge of the values of optical cross sections is fundamental for other quantitative analyses; for example, a calculated value of the absorption cross section for CdSe NWs has been used to estimate the quantum yield of their photoluminescence.[17] Consequently, absolute values of the absorption cross sections of both CdTe and CdSe NWs in a solution have been reported[18] for a couple of wavelengths. Furthermore, the polarization anisotropy of CdSe and CdSe/CdS core/shell NWs has been analyzed for two different wavelengths,[19] and even experimental polarization-dependent absolute values of the absorption cross section of CdSe NWs for one wavelength have been published.[20] These experimentally obtained absolute values are in good agreement with those obtained by Mie theory. So far, a profound analysis of the optical properties of individual NWs is available for germanium.[21] In comparison to Ge, Si has a smaller extinction coefficient k for the whole visible spectrum, that is, for wavelengths larger than ~340 nm.[22] This should, in principle, result in even stronger resonances. The same line of thought applies for the direct semiconductors[22] since they have, depending on the wavelength, either very high extinction coefficients k or extinction coefficients close to zero. The latter, of course, would rule out strong absorption, and thus, even strong resonant enhancement would still result in very low absorption efficiencies. Very recently, some optical properties, such as light absorption of NWs of different materials including silicon, have been published[23] and the basic physical principles are described that are responsible for the generality of resonances in one-dimensional nanostructures and that indicate which resonances are mostly suited for absorption and how absorption depends

*Address correspondence to gerald.broenstrup@gmail.com.

Received for review May 9, 2010 and accepted November 04, 2010.

Published online November 16, 2010.
10.1021/nn101076t

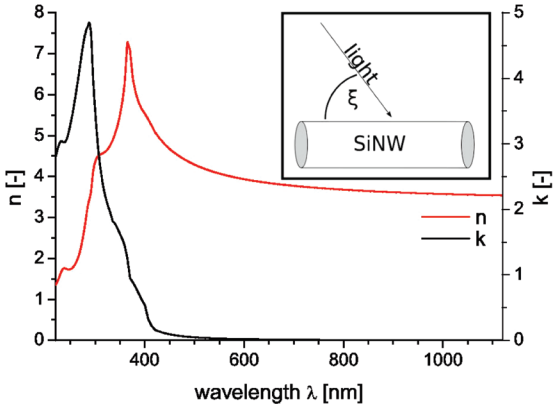

Figure 1. Complex refractive index $\tilde{n} = n + ik$ of silicon given by the refractive index n and the extinction coefficient k taken from ref 24. Inset: Schematics of SiNW position with respect to the incident illuminating light: definition of the angle of light incidence ξ.

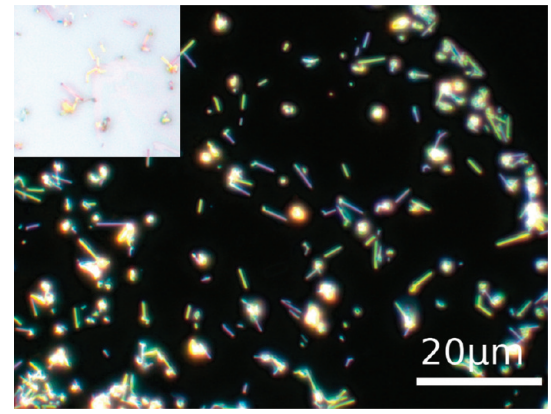

Figure 2. Optical micrograph of SiNWs on a glass substrate using a dark-field illumination configuration. Thus, only the scattered light is visible. The different colors of the SiNWs indicate that SiNWs of different diameters scatter the light differently. Inset: bright-field image of SiNWs on a glass substrate; in this case, only the transmitted light is visible. SiNWs are visible with an optical microscope because they scatter light efficiently despite their nanometer scale.

on the geometrical cross section of the SiNWs. Moreover, this paper describes how several rectangular NWs of amorphous Si lying in parallel can enhance the light absorption compared to a thin film.

However, both a detailed analysis of the scattering behavior of SiNWs and an analysis of the polarization dependence of the optical properties of SiNWs are still missing. Here, the present paper will contribute new experimental data of polarization and illumination controlled bright- and dark-field optical analyses together with analytical Mie calculations, contributing the polarization-dependent absorption efficiencies Q_{abs} of individual SiNWs. The dependence of scattering and absorption on the diameter d of SiNWs, on the wavelength λ of the illuminating light, on its angle of incidence ξ and on the polarization is discussed. The angle of incidence ξ is the angle between the illuminating light and the long axis of the SiNW, as schematically shown in the inset of Figure 1. Our findings show that absorption and scattering efficiencies are strongly dependent on the wavelength λ of the illuminating light, its polarization, and the diameters d of the SiNWs. These findings indicate that SiNWs are ideal candidates for a sensitive tuning of photonic devices by varying certain parameters of the SiNWs, such as the diameter and orientation with respect to the incident light.

To calculate scattering and absorption efficiencies Q_{sca} and Q_{abs}, the well-known Mie theory[16] is used. The efficiencies Q_{sca} and Q_{abs} are dimensionless and defined by the ratio of the particular cross section C_{sca} or C_{abs} and the geometrical area A of the object, $Q_{sca/abs} = C_{sca/abs}/A$. The cross section is defined as an imagined area around the illuminated object. As soon as an illuminating beam hits this area, interaction will occur. Within the limits of geometrical optics, this means the absorption cross section C_{abs} of a hypothetical, perfectly absorbing black body is always equal to the geometrical area A of the object and thus the absorption efficiency Q_{abs} always equals 1—independently of the geometrical shape. For a body that is an imperfect absorber, the absorption efficiency Q_{abs} resides between 0 and 1. Furthermore, within the limits of geometrical optics, the efficiencies Q are, in general, limited to values between 0 and 1. Leaving these limits of geometrical optics, as occurs when structures smaller than the illuminating wavelength λ are illuminated, such as the SiNWs in our experiments, different findings concerning the cross sections can occur (*e.g.*, absorption efficiencies Q_{abs} much bigger than 1). This means that absorption cross sections, C_{abs}, are bigger than the geometrical area A of the object; that is, the SiNW can thus collect light from an area much bigger than its geometrical area A (*i.e.*, the area covered by the SiNW itself). A similar effect has been calculated for an array consisting of SiNWs with a diameter $d = 200$ nm and a length of 2000 nm embedded in a polymer matrix for one wavelength $\lambda = 350$ nm.[8] In analogy to the absorption efficiencies Q_{abs} bigger than 1 outside of the framework of geometrical optics, scattering efficiencies Q_{sca} bigger than 1 can occur, which means in this case that light is scattered from an area bigger than the geometrical area A of the SiNW. In our examples, the calculated scattering efficiencies Q_{sca} reach values up to 901% and the absorption efficiencies Q_{abs} reach values of up to 449%. This shows that SiNWs have the potential to harvest and scatter light very effectively.

RESULTS

Optical Microscopy. SiNWs lying flat on a glass substrate show a broad spectrum of different colors (*cf.* Figure 2) as presented in optical micrographs in both dark-field and bright-field geometry. Each straight SiNW shows only one color, except the end points or when other particles are lying very close to the SiNW. The investigated SiNWs are several times longer than the wavelength of the illuminating light in vacuum. The ef-

fective wavelength of the light in the SiNWs is about 3.5 times smaller. Therefore, we do not consider the length of the SiNWs important for resonances, which could lead to different colors. These resonances would be considerably damped over such distances in Si. Hence, we assume that different colors point to different SiNW diameters.

To further analyze the cause of these different colors of individual SiNWs, the diameters of some of these SiNWs are measured using a scanning electron microscope (SEM) (*cf.* insets in Figure 3). The relation to the optical dark-field measurements that show the different colors is maintained by making use of markers that can be identified in the SEM as well as in the optical microscope. The color of the SiNWs in the optical microscope images is clearly correlated to the diameters *d* of the SiNWs (*cf.* insets in Figure 3). SiNWs with colors ranging all over the visible spectrum can be found. The correlation of SiNW diameter measurements and the color analysis with an optical microscope shows that a change in SiNW diameter *d* from 77 to 118 nm is responsible for a color change of blue to orange in dark field. This finding suggests that the SiNW scattering or absorption can be tuned very sensitively by slightly varying the SiNW diameter. The aforementioned experimental findings are supported by analytical Mie calculations[16] of the scattering efficiencies Q_{sca}.

Scattering Efficiencies Q_{sca} Based on Mie Theory. The colors of individual SiNWs in dark field and their diameters *d* as obtained by SEM measurements can be related to the scattering efficiencies Q_{sca} from Mie calculations (Figure 3). The colors of SiNWs vary with their diameters *d* since the intensity of the scattered light is proportional to the product of the intensity of the illuminating light and the scattering efficiencies Q_{sca}. Q_{sca} is dependent not only on the wavelength of the incident light but also on the diameter *d* of the SiNWs. As shown in Figure 3, the colors of individual SiNWs obtained from optical dark-field microscopy very well coincide with the colors that are expected from the Mie theory calculations. For example, SiNWs with a diameter of $d =$ 77 nm show big scattering efficiencies Q_{sca} for blue light and thus appear blue in the corresponding optical dark-field image, or SiNWs with a diameter of $d =$ 107 nm appear yellow in optical dark-field microscopy according to a scattering efficiency peak at a wavelength of yellow light.

Scattering Spectra. To quantitatively analyze the scattering behavior of the SiNWs, including the dependence on the polarization, scattering spectra with polarized, transmitted (*i.e.*, the SiNWs are illuminated through the glass substrate) light are taken in dark-field configuration. The positions of the peaks in the measured spectra are in accordance with the corresponding Mie calculations (*cf.* Figure 4, Figure 5, and Figure 6), and the spectra show pronounced polarization dependence.

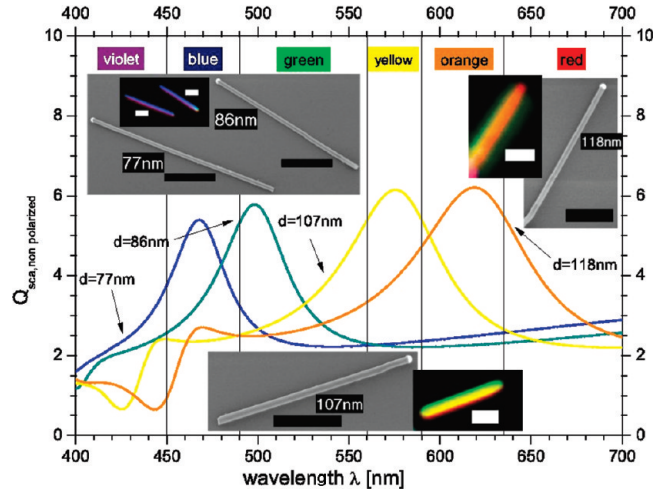

Figure 3. Scattering efficiencies Q_{sca} depending on SiNW diameters *d* calculated using Mie theory for perpendicular illumination ($\xi = 90°$) with nonpolarized light. Insets: SEM images and corresponding dark-field light optical micrographs of individual SiNWs lying flat on a glass substrate; all scale bars represent 1 μm; the SiNW diameters *d* are labeled in the SEM micrographs; the error for these values ranges from 5 to 8 nm, for the 77 and 118 nm diameter, respectively. The optical dark-field images superimposed with the calculated scattering efficiency Q_{sca} show a very good agreement.

Any illuminating electromagnetic field can be split into two independent polarizations. For the so-called transversal electric (TE) polarization, the vector of the magnetic $\vec{H}$-field is parallel to the SiNW's long axis, and for the so-called transversal magnetic (TM) polarization, the vector of the electric $\vec{E}$-field is parallel to the SiNW's long axis. The ratio of the intensities of the spectra measured with TE and TM polarized light, however, shows differences with respect to the ratio of the calculated scattering cross sections $Q_{sca,TE}/Q_{sca,TM}$ (*cf.* Figure 5 and Figure 6). In particular, the TE polarized light is scattered much stronger compared to the TM polarized light than predicted by the Mie calculations. This may be interpreted as an influence of the substrate, given that the substrate is not considered in the Mie calculations of the scattering efficiencies Q_{sca}. Though the background of the scattered light from the substrate does not show any pronounced peaks, the interaction between a SiNW and the substrate could lead to new patterns in the scattering spectrum. Spectra taken without polarizer show these differences between experimental measurements and Mie calculations, as well (*cf.* Figure 4).

Calculations of Scattering and Absorption Efficiencies of Individual SiNWs Based on Mie Theory. ***Scattering Efficiencies for Perpendicular Illumination $\xi = 90°$.*** As shown in Figure 4, Figure 5, and Figure 6, the scattering cross sections Q_{sca} do strongly depend on the wavelength λ of the illuminating light and its polarization, thus permitting to tune light scattering in SiNWs for device applications, though if the SiNWs are not embedded in a homogeneous medium the effects of the close (*i.e.*, distances comparable to a few times the wavelength λ) surrounding have to be considered.

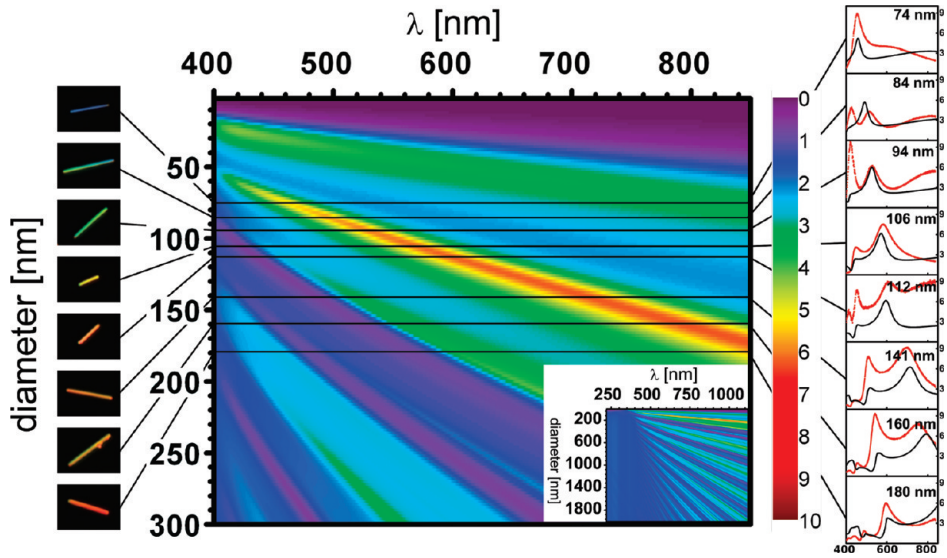

Figure 4. Calculated scattering efficiencies Q_{sca} for nonpolarized light at normal incidence ($\xi = 90°$) for $d = 2$ and 300 nm and $\lambda = 400$ and 850 nm. Solid black lines indicate the positions of the measured spectra. On the right-hand side, normalized measured scattering spectra are shown (red lines), and the black lines in these graphs are the corresponding calculated scattering efficiencies Q_{sca}. The measured and normalized (following eq 10) scattering intensities are scaled with a constant factor for each SiNW to match the calculated scattering efficiencies Q_{sca}. Thess factors are the same for every polarization shown in Figure 4, Figure 5, and Figure 6. The diameters of the SiNW shown in the graphs are measured using an AFM. The scale on the right-hand side shows the scattering efficiencies. On the left side, optical dark-field micrographs of the corresponding SiNWs are shown. Inset: Q_{sca} for $d = 2$ and 2000 nm and $\lambda = 220$ and 1120 nm.

For illumination with wavelengths smaller than ~360 nm, such as for ultraviolet light, the scattering efficiencies Q_{sca} do not show a strong dependence on the diameters of the SiNWs (*cf.* insets in Figure 4, Figure 5, and Figure 6). This is in line with the direct band gap of Si,[25] which resides at 3.4 eV ($\lambda = 365$ nm). In consequence of this, Si has a very high extinction coefficient k below wavelengths smaller than ~360 nm (*cf.* Figure 1). This results in a mean free path of light in Si of only a few nanometers for these wavelengths effectively suppressing resonant enhancement effects.

For wavelengths larger than ~400 nm, Q_{sca} shows a branched structure for both TE and TM polarization. The branches of high Q_{sca} are nearly straight lines in the plotted (λ, d)-plane (*cf.* Figure 4, Figure 5, and Figure 6). The slope of the branches is decreasing with increasing diameters d and decreasing wavelengths λ. The number of these branches for a given diameter d is increasing with increasing diameter d. This branched structure accounts for effective scattering of only one optically active SiNW at different incident wavelengths. The occurrence of such a branched structure can be ex-

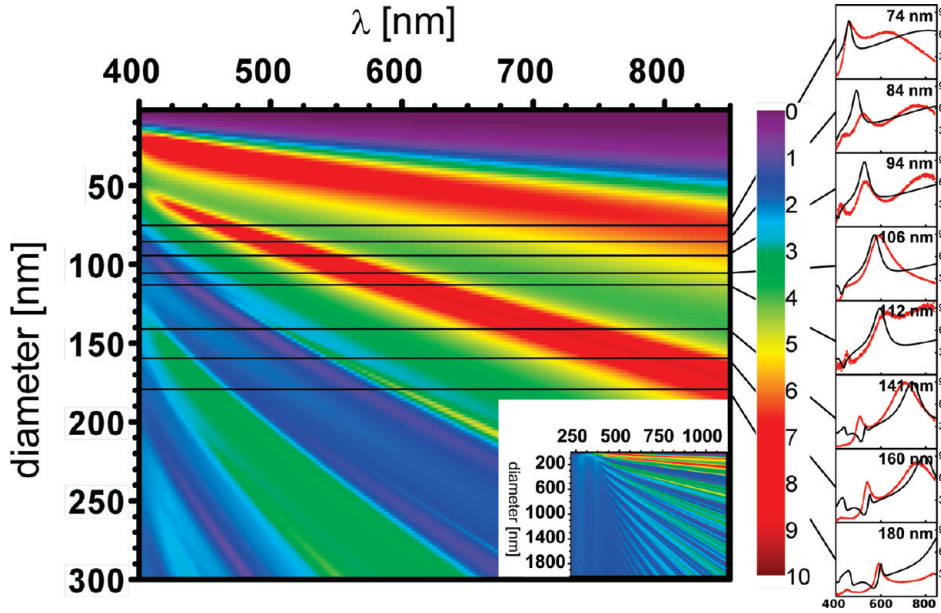

Figure 5. Same scattering efficiencies Q_{sca} as in Figure 4 for TM polarized light.

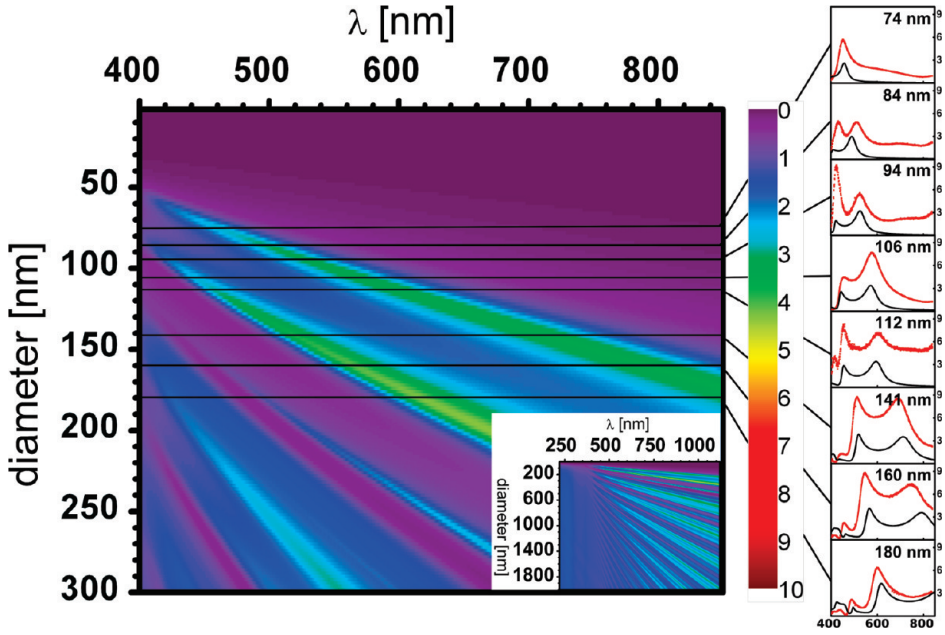

Figure 6. Same scattering efficiencies Q_{sca} as in Figure 4 for TE polarized light.

plained based on the analytical expressions for $Q_{sca}(\xi = 90°)$ as given by:[16]

$$a_i = \frac{\tilde{n}J_i(\tilde{n}x)J_i'(x) - J_i'(\tilde{n}x)J_i(x)}{\tilde{n}J_i(\tilde{n}x)H_i^{(1)\prime}(x) - J_i'(\tilde{n}x)H_i^{(1)}(x)} \quad (1)$$

$$b_i = \frac{J_i(\tilde{n}x)J_i'(x) - \tilde{n}J_i'(\tilde{n}x)J_i(x)}{J_i(\tilde{n}x)H_i^{(1)\prime}(x) - \tilde{n}J_i'(\tilde{n}x)H_i^{(1)}(x)} \quad (2)$$

$$x = \frac{2\pi}{\lambda}\frac{d}{2} \quad (3)$$

$$\tilde{n} = n + ik \quad (4)$$

$$Q_{sca,TM} = \frac{2}{x}\left[|b_0|^2 + 2\sum_{i=1}^{\infty}|b_i|^2\right] \quad (5)$$

$$Q_{sca,TE} = \frac{2}{x}\left[|a_0|^2 + 2\sum_{i=1}^{\infty}|a_i|^2\right] \quad (6)$$

Here $\tilde{n} = n + ik$ is the already mentioned complex refractive index, J_i is the Bessel functions of first kind of order i, and $H^{(1)}$ is the Hankel functions of first kind of order i. The scattering efficiencies Q_{sca} for perpendicular illumination $\xi = 90°$ are only dependent on terms like $x = d\pi/\lambda$ and $x\tilde{n}$. Since the complex refractive index $\tilde{n} = n + ik$ of silicon shows only a weak dependence on the wavelength λ for $\lambda > 500$ nm (*cf.* Figure 1), these terms are nearly proportional to d/λ. Thus, the scattering efficiencies Q_{sca} are nearly constants for straight lines in the (λ, d)-plane. The highest values for Q_{sca} (up to 901%) can be found for TM polarized light in a branch defined by the points $d = 64$ nm, $\lambda = 425$ nm and $d = 230$ nm, $\lambda = 1100$ nm. Another branch with high scattering efficiencies Q_{sca} (up to 866%) for even thinner SiNWs is given by the points $d = 16$ nm, $\lambda = 370$ nm and $d = 62$ nm, $\lambda = 720$ nm.

Since these are very common diameters for SiNWs,[2,26] it is possible to use this knowledge to optimize the growth of SiNWs using the particularly large scattering efficiencies Q_{sca} by controlling the SiNW diameters. The assessment of the SiNW diameters can be carried out by determination of the colors of the SiNWs in an optical microscope in dark-field configuration (*cf.* Figure 3). The scattered light analysis can, in principle, be used for *in situ* monitoring of the SiNWs' diameters, when they are individually grown in place in future devices. This *in situ* control during the SiNW growth can be decisive for successfully producing SiNW-based devices since *ex situ* diameter control is normally associated with oxidation of the SiNWs, which can prevent further epitaxy on the SiNWs.[27] An *in situ* control of the diameter could be necessary since not only the optical properties but also the electrical properties of SiNWs are strongly dependent on the diameter.[28] It also provides the option for a fast and low-cost *ex situ* diameter SiNW control to be used when implementing SiNWs in future device concepts. This can even be double checked by measuring the different scattering intensities for the different polarizations. Encouraging for a further use of this method is that the polarization dependence of the scattering efficiencies has already successfully been used with one wavelength ($\lambda = 1548$ nm) to measure the displacement of SiNWs.[26] The minima and maxima of the scattering efficiencies Q_{sca} can be a knowledge that may be important to minimize or maximize the scattering of light for optical SiNW-based sensors.

Absorption Efficiencies for Perpendicular Illumination $\xi = 90°$. The absorption efficiencies Q_{abs} are again a dimensionless number and are about 1 order of magnitude lower

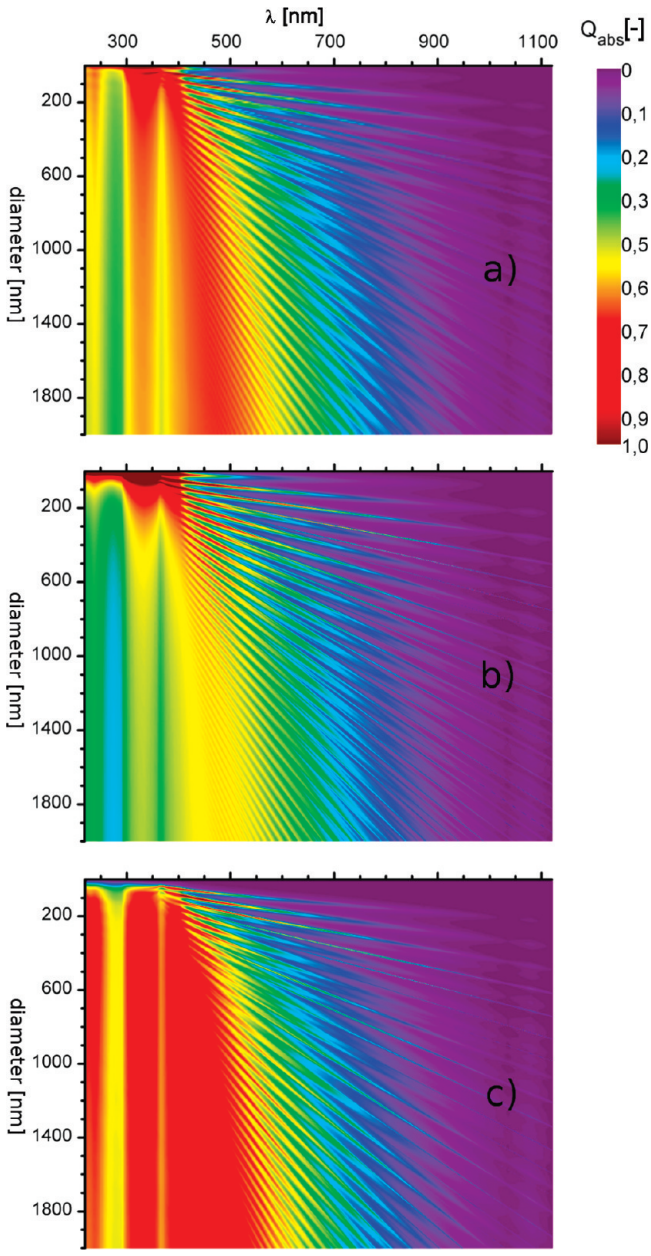

Figure 7. Absorption efficiencies Q_{abs} for d = 2 and 2000 nm and λ = 220 and 1120 nm for (a) nonpolarized light, (b) TM polarized light, and (c) TE polarized light.

than the scattering efficiencies Q_{sca}. This is not surprising because Si is an indirect band gap semiconductor. Note that the color scale implies 0 to 1 for Q_{abs} (Figure 7) and 0 to 10 for Q_{sca} (Figure 4, Figure 5, and Figure 6).

The results for the nonpolarized light (Figure 7a) are in accordance with those published in ref 23. However, in ref 23, it is mentioned that nanowires with diameters bigger than 100 nm do not show pronounced polarization dependence. This is only in qualitative accordance with our calculations; that is, the branches with high Q_{abs} are more or less at the same position in the (λ, d)-plane for the different polarizations, but the values of Q_{abs} show strong polarization dependence for all calculated diameters (*cf.* Figure 7).

The absorption efficiencies Q_{abs} show for λ < 360 nm (corresponding to the smallest direct band gap in Si[25]) only a weak dependence on the diameter d. Here, the direct band gap character of the Si with a high extinction coefficient k is dominating. Even though for larger wavelengths λ, Si is an indirect semiconductor, high absorption efficiencies Q_{abs} are possible because of resonant enhancement effects occurring in the SiNWs. These resonant enhancement effects are restricted to certain wavelengths and diameters, building the basis for a complex branched structure, similar to the structure of the scattering efficiencies Q_{sca} shown before.

A way to use SiNWs as wavelength- and polarization-sensitive photodetectors is as follows. Absorbed photons can produce free carriers in the SiNWs. Consequently, the conductance of undoped SiNWs rises proportional to the absorbed energy of light. Since SiNWs absorb light very specific with respect to the wavelength and polarization of incident light, the photoresistance is as very specific to these properties of the incident light. This method has been used for germanium NWs[21] and very recently as well for SiNWs.[23]

By examining the structure of the branches of high absorption efficiencies Q_{abs}, we find that the slope of the branches decreases for increasing diameters d and decreasing wavelengths λ, and these branches are nearly straight lines. These findings are very similar to what was found for the scattering efficiencies Q_{sca}. This is not surprising when looking at the formula for perpendicular illumination ξ = 90° for Q_{abs}:

$$Q_{abs,TM} = \frac{2}{x}\Re[b_0 + 2\sum_{i=1}^{\infty} b_i] - Q_{sca,TM} \qquad (7)$$

$$Q_{abs,TE} = \frac{2}{x}\Re[a_0 + 2\sum_{i=1}^{\infty} a_i] - Q_{sca,TE} \qquad (8)$$

The terms x, b_0, a_0, $Q_{sca,TM}$, and $Q_{sca,TE}$ have the same meaning as in eq 1−6. $\Re$ is only the real part taken, and $Q_{abs,TM}$ and $Q_{abs,TM}$ are the absorption efficiencies for *TM* and TE polarized light, respectively. In the case of perpendicular illumination ξ = 90°, the absorption efficiencies Q_{abs} are only dependent on the terms such as Q_{sca}, (*i.e.*, $x = d\pi/\lambda$ and $x\tilde{n}$). This gives analogy to the arguments for Q_{sca} straight lines in the (λ, d)-plane for the absorption efficiencies Q_{abs}. Since Si is an indirect semiconductor, small wavelengths λ close enough to the direct gap are needed to obtain high absorption efficiencies Q_{abs}, despite the resonant enhancement effects. Note that for all 2 nm < d < 2000 nm calculated examples, Q_{abs} > 100% is restricted to wavelengths λ < 474 nm for TE polarized light and λ < 576 nm for TM polarized light. For diameters d smaller than 20 nm and ultraviolet light, the absorption efficiencies Q_{abs} are very different for the different polarizations. For wavelengths between 230 nm < λ < 1120 nm, Q_{abs} is always

smaller than 20% for TE polarized light, while it can reach values larger than 440% for TM polarized light ($Q_{abs,TM}(d = 12\ nm, \lambda = 365\ nm) = 449\%$). This opens up the opportunity to build very efficient nanoscale Si technology based polarization detectors. For larger diameters, the polarization dependence is about the opposite: for diameters d larger than 160 nm, Q_{abs} tends to be higher for TE polarized light than for TM polarized light (*cf.* Figure 7b,c). Furthermore, there is a general trend to higher Q_{abs} for larger diameters d for wavelengths between 380 nm $< \lambda <$ 1120 nm for both polarizations. This is again due to the indirect character of Si for these wavelengths, and it is critical for many optics applications such as solar cells, where the whole solar spectrum up to wavelengths corresponding to the gap of the semiconductor ($\lambda = 1120$ nm for Si[29]) should be absorbed.

For applying SiNWs in solar cell concepts, the following properties are important: For diameters d smaller than 120 nm and wavelengths λ larger than 700 nm, Q_{abs} is always smaller than 7%. For even larger wavelengths ($\lambda > 850$ nm), Q_{abs} does not exeed a comparable value ($Q_{abs} < 7.2\%$) for diameters d up to 200 nm. Although these values seem rather low, they can be sufficient if many SiNWs are used to absorb the light. This thought is supported by the fact that comparably large absorption of thin layers of SiNWs have already been reported.[11]

Note that commonly used multicrystalline Si wafer based solar cells have a thickness of a few hundred micrometers to absorb light from the entire solar spectrum sufficiently. Because of this thickness large charge, carrier diffusion lengths are needed and, consequently, very pure low defective and thus expensive Si is needed. The enhancement of light absorption of SiNWs with respect to Si thin films becomes even more obvious when they are directly compared. For infrared light ($\lambda = 850$ nm), a SiNW with a diameter of 172 nm shows an absorption efficiency $Q_{abs} = 5.37\%$ for nonpolarized light. The absorption $Abs_{bulk\text{-}Si}$ of a Si thin film with the same thickness $z = 172$ nm, even with no reflection at all, can be estimated following the Beer−Lambert law

$$\begin{aligned} Abs_{bulk\text{-}Si} &= 100\% - e^{(-z4\pi k/\lambda)} \\ &= 100\% - e^{(-172\ nm \times 4 \times \pi \times 4.05 \times 10^{-3}/850\ nm)} \\ &= 1.02\% \end{aligned} \quad (9)$$

Here k is the extinction coefficient for $\lambda = 850$ nm, $k(850\ nm) = 4.05 \times 10^{-3}$. The absorption efficiency $Q_{abs} = 5.37\%$ of the SiNW is more than five times higher than the absorption $Abs_{bulk\text{-}Si} = 1.02\%$ of the Si thin film with a perfect anti-reflective coating.

Dependence of the Scattering Efficiencies on the Angle of Incident ξ. Since the angle of incidence ξ is not always 90°, we will discuss how the optical properties are changing when the angle of incidence ξ is changed. Especially, if SiNWs are grown on an amorphous substrate like glass, they will be orientated randomly and all sorts of oblique orientations with respect to the substrate surface normal can occur. Consequently, the angle of incidence ξ will be randomly distributed.

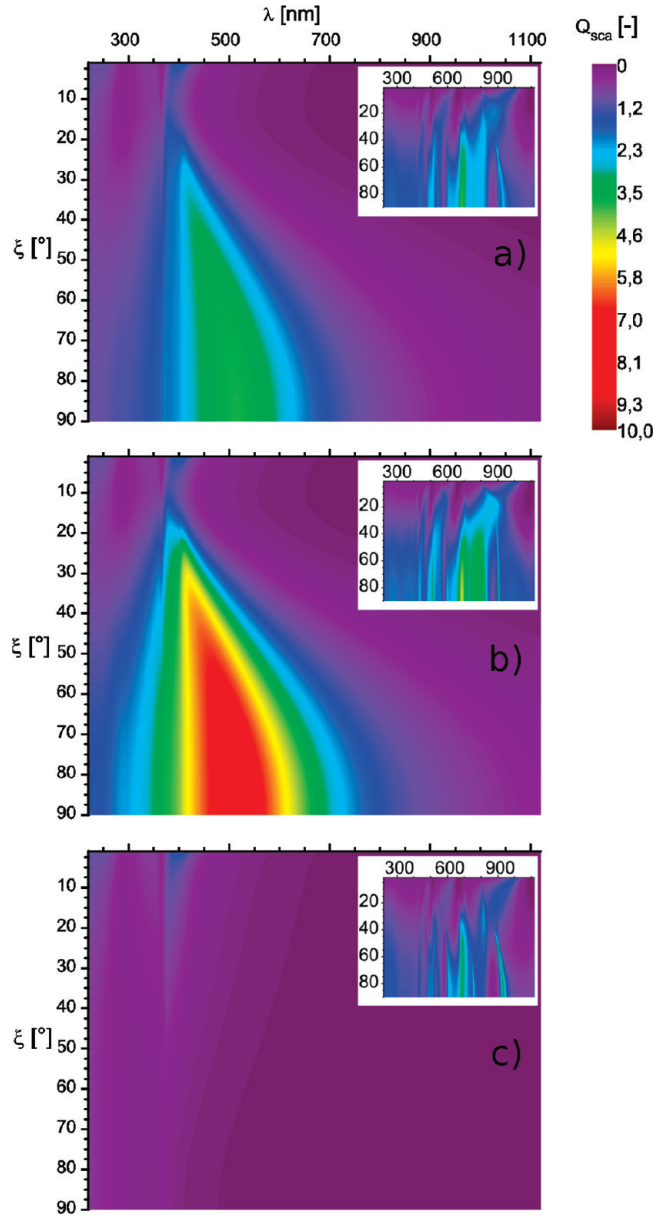

Figure 8. Scattering efficiencies Q_{sca} for a SiNW with a diameter d = 40 nm and λ = 220 and 1120 nm for different angles of illumination ξ for (a) nonpolarized light, (b) TM polarized light, and (c) TE polarized light. Insets: same for a SiNW with a diameter d = 400 nm.

A statistical approach based on the more simplified Rayleigh-type model to calculate the reflectance of thin films of SiNWs has been applied quite successfully by Street and co-workers.[10] The calculations shown in this paper can be used as a basis for more precise calculations of the optical properties of SiNW thin films composed of ensembles of randomly distributed SiNWs. For the discussion of the dependence on the angle of incidence ξ, two typical examples are chosen.

In the first example, a SiNW with a diameter $d = 40$ nm is illuminated. For perpendicular illumination (ξ =

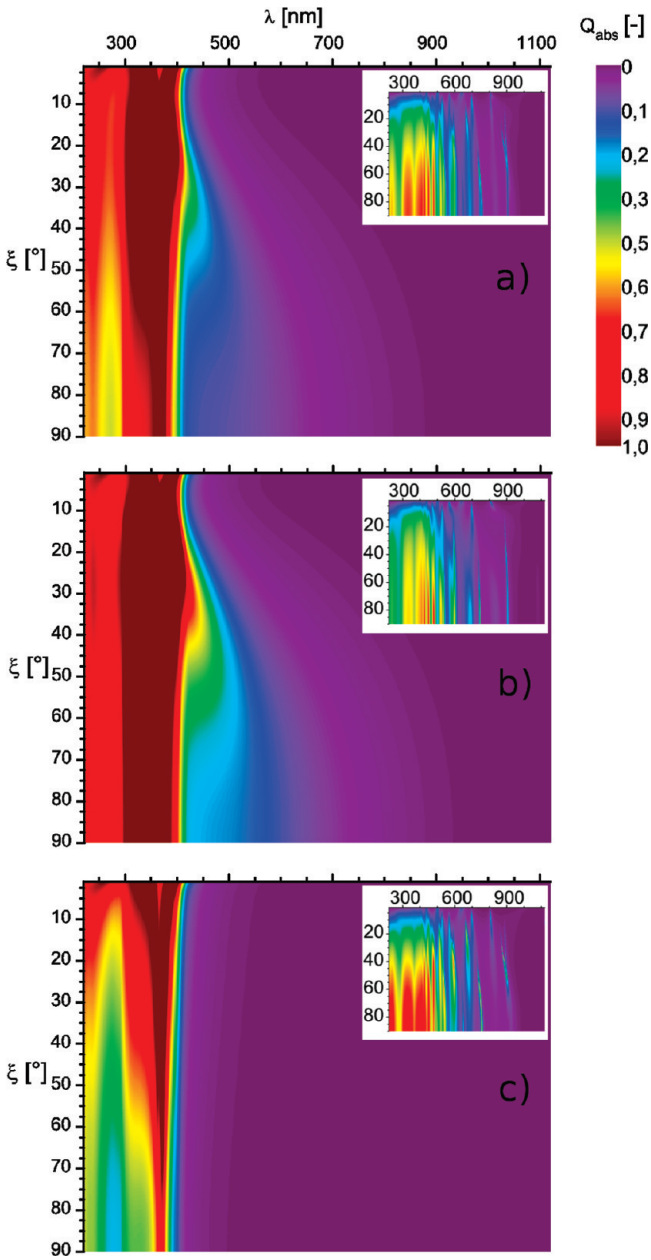

Figure 9. Absorption efficiencies Q_{abs} for a SiNW with a diameter d = 40 nm and λ = 220 and 1120 nm for different angles of illumination ξ for (a) nonpolarized light, (b) TM polarized light, and (c) TE polarized light. Insets: same for a SiNW with a diameter d = 400 nm.

90°), it can be seen that scattering efficiency Q_{sca} does not show a very strucutured dependence on the wavelength λ; that is, there is only one branch in the (λ, *d*)-plane for TM polarized light (*cf.* Figure 5) and none for TE polarized light (*cf.* Figure 6); however, for the TM polarization, the branch covers a large part of the visible spectrum of light for perpendicular illumination (ξ = 90°). This branch is getting much narrower for smaller ξ (*cf.* Figure 8b). On the other hand, there is no such branch in the (λ, *d*)-plane for TE polarized light for perpendicular illumination (ξ = 90°). In this case, Q_{sca} is increasing for decreasing ξ for wavelengths λ smaller than 450 nm, up to Q_{sca} = 2.1 for ξ = 1° and λ = 406 nm (*cf.* Figure 8c). Conclusively, it can be stated that the qualitative properties do not change drastically if the angle of incidence ξ is not altered too much. This is encouraging for further engineering of devices using SiNWs because it is not necessary to calibrate the angle of incidence ξ very precisely.

The second example uses the illumination of a *SiNW* with a diameter of d = 400 nm. In this case, there are many branches in the (λ, *d*)-plane for perpendicular illumination (ξ = 90°) for both polarizations (*cf.* insets in Figure 5 and Figure 6). The branches change with ξ in different ways. For TE polarization, some branches bend to smaller wavelengths λ for smaller ξ (*cf.* inset in Figure 8c), while for the TM polarization, most branches do not show such a behavior (*cf.* inset in Figure 8b). In summary, this gives a rather complicated quantitative dependence of Q_{sca} on λ and ξ. Again, it can be stated that the qualitative optical properties such as light scattering do not change dramatically when the angle of incidence ξ is not altered too much. Since it is still a challenge to build devices based on SiNWs, it is encouraging that the angle of incidence ξ is not very critical, and thus engineering of devices does not require intensive control of this parameter.

For bigger diameters (d > 400 nm), the dependence of optical properties on the angle of incidence ξ of incident light is qualitatively the same but in detail even a bit more complex.

Dependence of the Absorption Efficiencies on the Angle of incident ξ. To discuss the dependence of the absorption efficiencies Q_{abs} on the angle of incidence ξ, the same two examples have been chosen that are used to discuss the dependence of Q_{sca} on ξ.

The first example is a SiNW with a diameter of d = 40 nm. For perpendicular illumination (ξ = 90°), one branch can be seen in the (λ, *d*)-plane for both TM polarized light (*cf.* Figure 7b) and TE polarized light (*cf.* Figure 7c). For TM polarized light, there is a broad branch with Q_{abs} > 1 for nearly all angles of incidence ξ for wavelengths λ between 300 and 400 nm (*cf.* Figure 8b). For TE polarized light, Q_{abs} tends to have bigger values for smaller angles of incidence ξ for wavelengths λ smaller than 450 nm. For λ > 450 nm, Q_{abs} is smaller than 6% for all calculated angles of incidence ξ (*cf.* Figure 9c). As mentioned before, the qualitative course of the absorption efficiencies is not very strongly dependent on the angle of incidence ξ. The underlying physics of this behavior is that these small SiNWs act like simple dipoles with respect to incident light.[23]

For potential applications, this finding is advantageous since not much attention has to be paid to focus light on the SiNWs and small angles of incidence are sufficient so that it is possible to focus light on potential devices with cheap, small focal lengths lenses without losing potential predesigned tuning to certain wavelengths.

SiNWs with a diameter $d = 400$ nm show many branches in the (λ, d)-plane for perpendicular illumination ($\xi = 90°$) for both polarizations (*cf.* Figure 7). The branches show the trend that they become increasingly narrow for smaller ξ (*cf.* insets in Figure 9). In addition, there are a few small branches starting at angles different from $\xi = 90°$. This shows that for thicker SiNWs the situation becomes more complicated and the angle of illumination ξ has a stronger influence and thus needs to be more thoroughly considered when building wavelength-sensitive SiNW-based devices.

CONCLUSION

The scattering and absorption efficiencies of SiNWs are calculated using Mie theory depending on polarization as well as the angle of incidence of the illuminating light and the diameters of the SiNWs. Quantitatively, these efficiencies depend strongly on the polarization of the incident light. The scattering efficiencies are generally higher for TM polarized light. The general trend for the absorption efficiencies is more complex. For TM polarized light, the absorption efficiencies are only higher than those for TE polarized light for SiNWs with diameters smaller than ~160 nm. For thicker SiNWs, the opposite holds true. The dependence of these cross sections on the angle of incidence ξ is not very pronounced. Calculated dependencies of scattering and absorption efficiencies very well coincide with experimental findings of scattering of white light in an optical microscope, which results, depending on the diameter of the SiNW, in a differently colored appearance of the SiNWs. The combined experimental and theoretical study of optical properties of individual SiNWs reveals a huge potential of SiNWs to be used as sensitively tunable building blocks in opto-electronic devices such as sensors, solar cells, and photodetectors.

METHODS

Preparation of Samples. The SiNWs are grown on Si wafers following the vapor−liquid−solid mechanism (VLS).[30] The Si is supplied by chemical vapor deposition (CVD) from a silane precursor in argon as the carrier gas at a mixture of 1:1 and a total pressures of 2.0 mbar. The one-dimensional wire growth is catalyzed by commercially available gold colloids (British Biocell Int.[31]). The use of gold colloids as catalysts for the SiNW growth has the potential to gain a certain control over the diameters of the SiNWs.[32] However, under different conditions during the CVD process, SiNWs with mixed diameters can occur due to gold diffusion.[33] Since the sample is placed about 1 mm above the heater, the absolute growth temperature on the wafer surface is unknown but could roughly be estimated to be around 500 °C based on pyrometer and thermocouple measurements.

After the CVD SiNW growth, the SiNWs are removed from the substrate by applying ultrasonic treatment for about 2 min with the sample residing in a small drop of isopropyl alcohol in a capsular. After the treatment, a SiNW isopropyl alcohol suspension is formed that is pipetted on a glass substrate. After drying of the suspension, dispersed, individual SiNWs can be found lying with their long axis flat on the glass substrate (*cf.* Figure 2).

Optical Measurements. The optical measurements are carried out with a Axio Imager (Zeiss Microimaging, Göttingen, Germany) optical microscope using as light source of a tungsten halogen lamp with a continuous spectrum with a color temperature of 3200 K. To experimentally obtain the scattering spectra of individual SiNWs, dark-field configuration is used. In this configuration, the direct light is blocked out and only the scattered light is passed through a pinhole to a spectrometer. The pinhole has a diameter of 100 μm and is coplanar to the real image plane of the tube lens. A multimode fiber is used to connect the pinhole to a Acton Research SpectraPro 2300i microspectrometer (Princeton Instruments, Trenton, NJ) with a grating with 150 lines and a peltier cooled CCD camera. With this setup, the scattered light of individual SiNWs is gathered. To obtain the scattering spectrum of a SiNW, the background from the glass substrate has to be removed and the spectrum has to be normalized with respect to the illuminating light source. This is done using the following equation:

$$I(\lambda)_{\text{normalized}} = \frac{I(\lambda)_{\text{NW,DF}} - I(\lambda)_{\text{BG,DF}}}{I(\lambda)_{\text{BG,BF}}} \quad (10)$$

where $I(\lambda)_{\text{NW,DF}}$ is the intensity of a NW, measured in dark-field (DF) configuration, $I(\lambda)_{\text{BG,DF}}$ is the intensity of the background (BG) of the sample without a NW, measured in dark-field configuration, and $I(\lambda)_{\text{BG,BF}}$ is the intensity of the light source, measured in bright-field (BF) configuration. Throughout this paper, we only show the normalized $I(\lambda)_{\text{normalized}}$ spectra.

Analytical Mie Calculations. For the calculation of efficiencies, Q_{sca} and Q_{abs}, using Mie theory, the following assumptions are made: The SiNWs are approximated by infinitely long cylinders with diameter d. These cylinders are assumed to be surrounded by air, which means that the surrounding medium is modeled as being nonabsorbing assuming a refractive index of $n = 1$. The SiNWs themselves are assumed to be composed of pure, undoped silicon with the complex refractive index $\tilde{n} = n + ik$ known for bulk silicon as plotted in Figure 1. Here n is the real part of the refractive index, k the extinction coefficient, and i the imaginary number. Values guiding the curve in Figure 1 for the complex refractive index are taken from ref 24.

The parameters that are varied for the Mie calculations are the diameter d of the SiNWs, the wavelength λ, the polarization, and the angle of incidence ξ (*cf.* inset in Figure 1) of the illuminating light. In this paper, efficiencies Q for diameters d ranging from 2 to 2000 nm are calculated. For the smallest diameters ($d < 5$ nm), quantum confinement effects are likely to occur.[34] This of course changes the complex refractive index $\tilde{n}$ of the SiNWs and thus the scattering and absorption efficiencies Q_{sca} and Q_{abs}. Our calculations do not account for quantum confinement effects. Therefore, calculations for SiNWs with diameters down to 5 nm can be done. However, the calculated efficiencies Q for $d < 5$ nm SiNWs based on the bulk refractive index data can be used to assess the influence of quantum confinement on the optical properties of these very thin SiNWs by comparing the measured values with the calculated ones. Furthermore, the calculated efficiencies Q can be used as a first approximation even for these very thin SiNWs.

The angle of incidence ξ is the angle between the long axis of the SiNW and the illuminating light, as schematically shown in the inset of Figure 1. The extreme cases are (i) perpendicular illumination, $\xi = 90°$, which means that the SiNWs are lying flat on an anticipated support/substrate while light is shining on the surface of this substrate perpendicularly, and (ii) parallel illumination, $\xi = 0°$, which means that the SiNWs are again lying on that support while the light is incident parallel to the SiNWs long axes. The latter extreme case ($\xi = 0°$) cannot be calculated in the framework of Mie theory because this case would imply that the top or buttom area of the SiNWs has to be considered. Since infinitely long SiNWs are assumed for the Mie calculations, the top and bottom areas are not considered and it is not possible to calculate the efficiencies for $\xi = 0°$ exactly but only for small angles of incidence ξ. In this paper, we restrict ourselves to a minimum angle of $\xi = 1°$.

The efficiencies of both absorption and scattering are first calculated for TE and TM polarized light. The corresponding efficiencies for nonpolarized light Q_{nonpol} can be calculated by averaging over the respective efficiencies for TM and TE polarized lights Q_{TM} and Q_{TE}:

$$Q_{nonpol} = \frac{1}{2}(Q_{TM} + Q_{TE}) \quad (11)$$

Acknowledgment. We thank F. Jahn for the scanning force microscopy measurements. Funding by the European Commission through the state of Thuringia within the project EFRE-SiFafl and ROD-SOL (FP7-NMP-227497) is gratefully acknowledged.

REFERENCES AND NOTES

1. Cui, Y.; Wei, Q.; Park, H.; Lieber, C. M. Nanowire Nanosensors for Highly Sensitive and Selective Detection of Biological and Chemical Species. *Science* **2001**, *293*, 1289–1292.
2. Cui, Y.; Zhong, Z.; Wang, D.; Wang, W. U.; Lieber, C. M. High Performance Silicon Nanowire Field Effect Transistors. *Nano Lett.* **2003**, *3*, 149–152.
3. Sivakov, V.; Andrä, G.; Gawlik, A.; Berger, A.; Plentz, J.; Falk, F.; Christiansen, S. H. Silicon Nanowire-Based Solar Cells on Glass: Synthesis, Optical Properties, and Cell Parameters. *Nano Lett.* **2009**, *9*, 1549–1554.
4. Kayes, B. M.; Atwater, H. A.; Lewis, N. S. Comparison of the Device Physics Principles of Planar and Radial p−n Junction Nanorod Solar Cells. *J. Appl. Phys.* **2005**, *97*, 114302–114312.
5. Tian, B.; Zheng, X.; Kempa, T. J.; Fang, Y.; Yu, N.; Yu, G.; Huang, J.; Lieber, C. M. Coaxial Silicon Nanowires as Solar Cells and Nanoelectronic Power Sources. *Nature* **2007**, *449*, 885–889.
6. Tsakalakos, L.; Balch, J.; Fronheiser, J.; Korevaar, B. A.; Sulima, O.; Rand, J. Silicon Nanowire Solar Cells. *Appl. Phys. Lett.* **2007**, *91*, 233117–233119.
7. Fang, H.; Li, X.; Song, S.; Xu, Y.; Zhu, J. Fabrication of Slantingly-Aligned Silicon Nanowire Arrays for Solar Cell Applications. *Nanotechnology* **2008**, *19*, 255703–255708.
8. Zhang, A.; You, S.; Soci, C.; Liu, Y.; Wang, D.; Lo, Y.-H. Silicon Nanowire Detectors Showing Phototransistive Gain. *Appl. Phys. Lett.* **2008**, *93*, 121110–121112.
9. Servati, P.; Colli, A.; Hofmann, S.; Fu, Y. Q.; Beecher, P.; Durrani, Z. A. K.; Ferrari, A. C.; Flewitt, A. J.; Robertson, J.; Milne, W. I. Scalable Silicon Nanowire Photodetectors. *Physica E* **2007**, *38*, 64–66.
10. Street, R. A.; Wong, W. S.; Paulson, C. Analytic Model for Diffuse Reflectivity of Silicon Nanowire Mats. *Nano Lett.* **2009**, *9*, 3494–3497.
11. Tsakalakos, L.; Balch, J.; Fronheiser, J.; Shih, M.-Y.; LeBoeuf, S. F.; Pietrzykowski, M.; Codella, P. J.; Korevaar, B. A.; Sulima, O. V.; Rand, J.; *et al.* Strong Broadband Optical Absorption in Silicon Nanowire Films. *J. Nanophotonics* **2007**, *1*, 013552–013561.
12. Muskens, O. L.; Borgstrom, M. T.; Bakkers, E. P. A. M.; Rivas, J. G. Giant Optical Birefringence in Ensembles of Semiconductor Nanowires. *Appl. Phys. Lett.* **2006**, *89*, 233117–233119.
13. Muskens, O. L.; Diedenhofen, S. L.; Kaas, B. C.; Algra, R. E.; Bakkers, E. P. A. M.; Gomez Rivas, J.; Lagendijk, A. Large Photonic Strength of Highly Tunable Resonant Nanowire Materials. *Nano Lett.* **2009**, *9*, 930–934.
14. Muskens, O. L.; Diedenhofen, S. L.; van Weert, M. H. M.; Borgström, M. T.; Bakkers, E. P. A. M.; Rivas, J. G. Epitaxial Growth of Aligned Semiconductor Nanowire Metamaterials for Photonic Applications. *Adv. Funct. Mater.* **2008**, *18*, 1039–1046.
15. Muskens, O. L.; Rivas, J. G.; Algra, R. E.; Bakkers, E. P. A. M.; Lagendijk, A. Design of Light Scattering in Nanowire Materials for Photovoltaic Applications. *Nano Lett.* **2008**, *8*, 2638–2642.
16. Bohren, C. F.; Huffman, D. R. *Absorption and Scattering of Light by Small Particles*; Wiley-VCH: Berlin, 1998.
17. Protasenko, V.; Hull, K.; Kuno, M. Disorder-Induced Optical Heterogeneity in Single CdSe Nanowires. *Adv. Mater.* **2005**, *17*, 2942–2949.
18. Protasenko, V.; Bacinello, D.; Kuno, M. Experimental Determination of the Absorption Cross-Section and Molar Extinction Coefficient of CdSe and CdTe Nanowires. *J. Phys. Chem. B* **2006**, *110*, 25322–25331.
19. Giblin, J.; Protasenko, V.; Kuno, M. Wavelength Sensitivity of Single Nanowire Excitation Polarization Anisotropies Explained through a Generalized Treatment of Their Linear Absorption. *ACS Nano* **2009**, *3*, 1979–1987.
20. Giblin, J.; Syed, M.; Banning, M. T.; Kuno, M.; Hartland, G. Experimental Determination of Single CdSe Nanowire Absorption Cross Sections through Photothermal Imaging. *ACS Nano* **2010**, *4*, 358–364.
21. Cao, L.; White, J. S.; Park, J.-S.; Schuller, J. A.; Clemens, B. M.; Brongersma, M. L. Engineering Light Absorption in Semiconductor Nanowire Devices. *Nat. Mater.* **2009**, *8*, 643–647.
22. Aspnes, D. E.; Studna, A. A. Dielectric Functions and Optical Parameters of Si, Ge, GaP, GaAs, GaSb, InP, InAs, and InSb from 1.5 to 6.0 eV. *Phys. Rev. B* **1983**, *27*, 985–1009.
23. Cao, L.; Fan, P.; Vasudev, A. P.; White, J. S.; Yu, Z.; Cai, W.; Schuller, J. A.; Fan, S.; Brongersma, M. L. Semiconductor Nanowire Optical Antenna Solar Absorbers. *Nano Lett.* **2010**, *10*, 439–445.
24. *Handbook of Optical Constants of Solids III*; Palik, E. D., Ed.; Academic Press: New York, 1998.
25. Phillips, J. C. Band Structure of Silicon, Germanium, and Related Semiconductors. *Phys. Rev.* **1962**, *125*, 1931–1936.
26. Nichol, J. M.; Hemesath, E. R.; Lauhon, L. J.; Budakian, R. Displacement Detection of Silicon Nanowires by Polarization-Enhanced Fiber-Optic Interferometry. *Appl. Phys. Lett.* **2008**, *93*, 193110–193112.
27. Lauhon, L. J.; Gudiksen, M. S.; Wang, D.; Lieber, C. M. Epitaxial Core−Shell and Core−Multishell Nanowire Heterostructures. *Nature* **2002**, *420*, 57–61.
28. Kimukin, I.; Islam, M. S.; Williams, R. S. Surface Depletion Thickness of p-Doped Silicon Nanowires Grown Using Metal-Catalysed Chemical Vapour Deposition. *Nanotechnology* **2006**, *17*, S240–S245.
29. Macfarlane, G. G.; McLean, T. P.; Quarrington, J. E.; Roberts, V. Fine Structure in the Absorption-Edge Spectrum of Si. *Phys. Rev.* **1958**, *111*, 1245–1254.
30. Wagner, R. S.; Ellis, W. C. Vapor−Liquid−Solid Mechansim of Single Crystal Growth. *Appl. Phys. Lett.* **1964**, *4*, 89–90.
31. http://www.britishbiocell.co.uk/.
32. Cui, Y.; Lauhon, L. J.; Gudiksen, M. S.; Wang, J.; Lieber, C. M. Diameter-Controlled Synthesis of Single-Crystal Silicon Nanowires. *Appl. Phys. Lett.* **2001**, *78*, 2214–2216.
33. Oehler, F.; Gentile, P.; Baron, T.; Ferret, P. The Effects of HCl on Silicon Nanowire Growth: Surface Chlorination and Existence of a 'Diffusion-Limited Minimum Diameter'. *Nanotechnology* **2009**, *20*, 475307–475312.
34. Ma, D. D. D.; Lee, C. S.; Au, F. C. K.; Tong, S. Y.; Lee, S. T. Small-Diameter Silicon Nanowire Surfaces. *Science* **2003**, *299*, 1874–1877.